doi:10.1017/S143192761600862X
Microsc. Microanal. 22 (Suppl 3), 2016


# Study of Direct Lithiation of Thin Si Membranes with Spatially-Correlative Low Energy Focused Li Ion Beam and Analytical Electron Microscopy Techniques

V.P. Oleshko[1], K.A. Twedt[2,3], C.L. Soles[1], J.J. McClelland[2]

[1] Material Measurement Laboratory and [2] Center for Nanoscale Science and Technology, National Institute of Standards and Technology, Gaithersburg, MD 20899
[3] Maryland Nanocenter, University of Maryland, College Park, MD 20742

Understanding and controlling defect interactions and transport properties of Li ions in silicon is crucial for the development of emerging technologies in energy storage and microelectronics [1-4]. With a theoretical energy storage capacity of ~4200 $mAhg^{-1}$, which is more than 10 times over than that of graphite (372 $mAhg^{-1}$), Si is an attractive anode material for high-performance Li-ion batteries [1, 4]. The practical use of Si-based anodes is, however, hampered by the large volumetric changes (up to ~400%) that occur during electrochemical charge/discharge cycling and the concomitant capacity fading. Further insights into fundamental mechanisms of Li-Si reactions are needed to address these problems. Here, we report on controlled low dose $Li^+$ ion implantation into 9 nm-thick amorphous (*a*-Si) membranes and 35 nm-thick single crystalline <100>-oriented (*c*-Si) membranes using a low-energy focused lithium ion beam ((LiFIB), FIG. 1a). With probe sizes of a few tens of nanometers at energies ranging from 500 eV to 6 keV and beam currents of a few pA, the LiFIB enables surface topography and composition sensitive imaging using ion-induced secondary electrons (*i*SE) and backscattered ions (BSI), respectively [5]. Furthermore, the LiFIB has a unique ability to implant certain amounts of $^7Li^+$ ions into any material with nanoscale precision, making it a potentially powerful tool for advanced battery materials research and material design via defect engineering and surface modification. In this work, we analyze the spatial distributions of lithium in the selected regions of the thin Si membranes where the low dose $Li^+$ ions were implanted through a combination of correlative low-energy LiFIB implantation/imaging, conventional and phase-contrast high-resolution transmission electron microscopy (CTEM/HRTEM), selected-area electron diffraction (SAED), scanning TEM (STEM), and electron energy-loss spectroscopic STEM imaging (EELS-STEM SI). This reveals information about the $Li^+$–Si interactions, bonding and lateral distributions of low $Li^+$ concentrations within the membranes in the range from $1\times10^3$ ion/$nm^2$ to $13\times10^3$ ion/$nm^2$ or from $1.1\times10^{-20}$ g/$nm^2$ to $14.6\times10^{-20}$ g/$nm^2$, respectively (FIGs. 1 and 2). It is noteworthy that this approach avoids the inherent electrochemical complications from the formation of an unstable solid-electrolyte interface (SEI) with poor conductivity. Through this approach we directly reveal the series of overlapping nanoscale physico-chemical processes that occur during the early stages of $Li^+$ implantation, including: (a) selective etching, amorphization and cracking of the Si membranes (FIGs. 1b and 2b); (b) the creation of interstitial-rich extended stepped and v-shaped defects (FIG. 2b); (c) clustering of mobile interstitials in tetragonal sites of the *c*-Si matrix (FIG. 2c) as well as (d) concentration gradient driven local diffusion of Li ions followed by (e) the formation of various mixed composition Si-Li alloy phases.

References:

[1] H. Kim, *et al*, J. Phys. Chem. C **114** (2010) 17942.
[2] E. Oliviero *et al*, J. Appl. Phys. **113** (2013) 083515.
[3] V.P. Oleshko, *et al*, Microsc. Microanal. **20** (Suppl 3) (2014) 426.
[4] V.P. Oleshko, *et al*, Nanoscale **6** (2014) 11756.
[5] K. A. Twedt *et al*, Ultramicroscopy **142** (2014) 24.

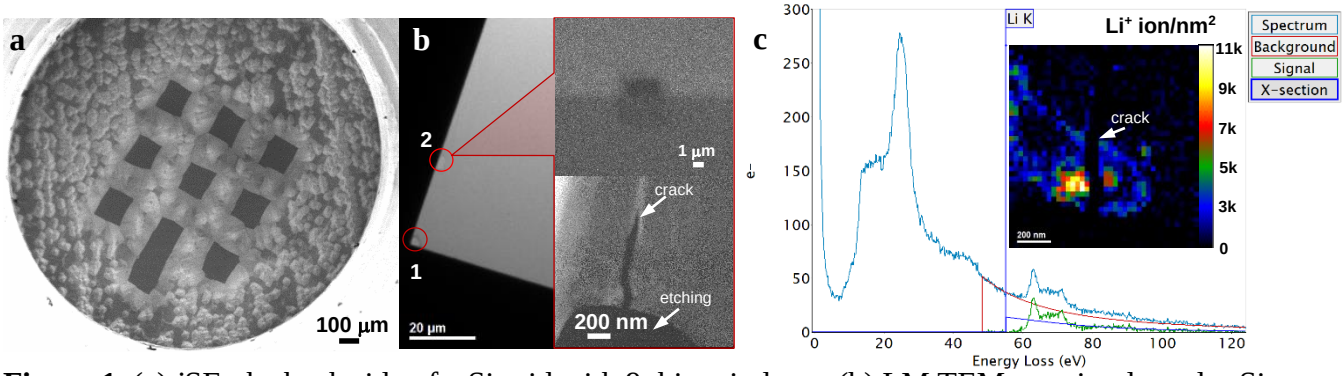


**Figure 1**. (a) *i*SE, the back side of a Si grid with 9 thin windows. (b) LM TEM, two implanted *a*-Si areas; *i*SE, a 2 x 4 µm rectangular implanted area 2, 30 min, *U*=4 kV, *I*≈1 pA (top), HAADF STEM (bottom), partial etching and cracking of a 9 nm-thick *a*-Si film due to the volume expansion. (c) EELS-STEM SI, low-loss EEL spectrum showing the Li K edge at 55 eV and the $Li^+$ areal density map (ion/$nm^2$, inset).

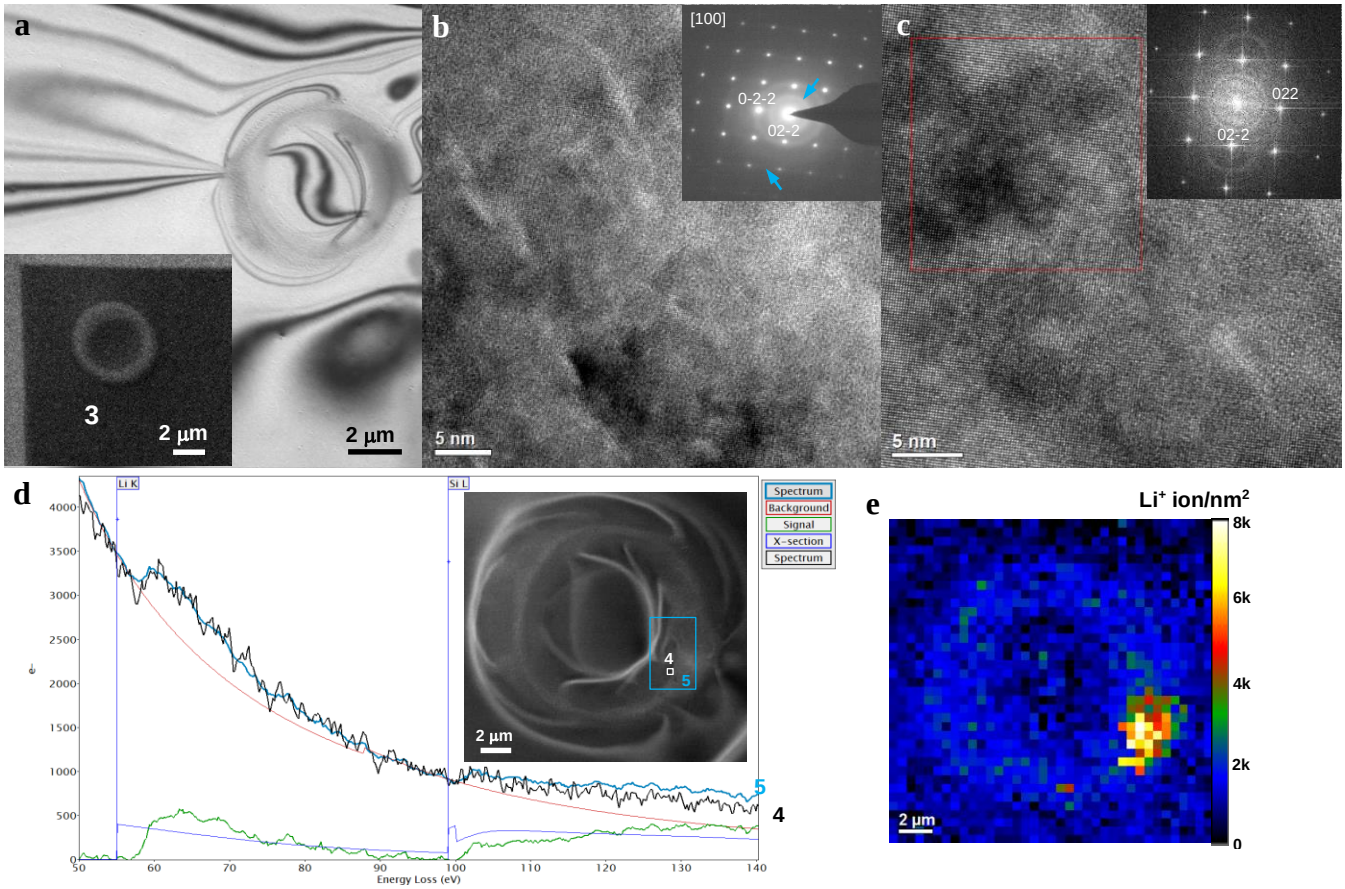


**Figure 2.** (a) *i*SE, 10 min, *U*=2 kV, *I*≈1 pA (inset) and BF-TEM images of a circular implanted area 3 in a 35 nm-thick *c*-Si film exhibiting stress-induced bending contours. (b, c) HRTEM, extended v-shaped and stepped $Li^+$-induced defects in the implanted area. The SAED pattern (inset) displays weak diffuse rings due to lithiated phases and diffuse intensity contours (blue arrows) in between the Bragg reflections caused by clustering of interstitials. (c) An interstitial-rich stepped defect. The FFT pattern (inset) from a red square reveals double diffraction rings from interstitials with 0.28 nm spacing along the [01$\bar{1}$] direction. (d, e) EELS-STEM SI, the area 3, normalized EEL spectra extracted from sites 4 and 5 (inset) which show the Li K edge at 55 eV and the Si $L_{2,3}$-edge at 99 eV. (e) The $Li^+$ areal density map (ion/$nm^2$).

https://doi.org/10.1017/S143192761600862X Published online by Cambridge University Press